https://doi.org/10.5194/essd-2023-36
Preprint. Discussion started: 24 February 2023

Open Access Earth System Science Data Discussions

A new habitat map of the Lena Delta in Arctic Siberia based on field and remote sensing datasets

Simeon Lisovski[1,*], Alexandra Runge[2,*], Iuliia Shevtsova[1], Nele Landgraf[3], Anne Morgenstern[2], Ronald Reagan Okoth[1,4], Matthias Fuchs[2], Nikolay Lashchinskiy[5,6], Carl Stadie[2,7], Alison Beamish[8], Ulrike Herzschuh[1,9,10], Guido Grosse[1,11], Birgit Heim[1]

[*] Both authors contributed equally

[1] Alfred Wegener Institute Helmholtz Centre for Polar and Marine Research, Polar Terrestrial Environmental Systems, 14473 Potsdam, Germany

[2] Alfred Wegener Institute Helmholtz Centre for Polar and Marine Research, Permafrost Research, 14473 Potsdam, Germany

[3] Humboldt University, Department of Geosciences, 12489 Berlin, Germany

[4] Julius-Maximilians Universität Würzburg, Institute of Geography and Geology, Oswald-Külpe-Weg 86, 97074 Würzburg, Germany

[5] Central Siberian Botanical Garden, Siberian Branch, Russian Academy of Sciences, Novosibirsk, 630090 Russia

[6] Trofimuk Institute of Petroleum Geology and Geophysics, Siberian Branch, Russian Academy of Sciences, Novosibirsk, 630090 Russia

[7] University of Greifswald, Institute for Geography and Geology, Germany (current address: University of Copenhagen, Department of Earth Science and Nature Management, Denmark)

[8] GFZ German Research Centre for Geosciences, Helmholtz Centre Potsdam.

[9] University of Potsdam, Institute of Environmental Sciences & Geography, Karl-Liebknecht-Str. 24-25, 14476 Potsdam, Germany

[11] University of Potsdam, Institute of Biochemistry and Biology, Karl-Liebknecht-Str. 24-25, 14476 Potsdam, Germany

[12] University of Potsdam, Institute of Geosciences, Karl-Liebknecht-Str. 24-25, 14476 Potsdam, Germany

Correspondence to: Simeon Lisovski (Simeon.Lisovski@awi.de)

https://doi.org/10.5194/essd-2023-36
Preprint. Discussion started: 24 February 2023

Abstract. The Lena Delta is the largest river delta in the Arctic (about 30 000 km2) and prone to rapid changes due to climate warming, associated cryosphere loss and ecological shifts. The delta is characterized by ice-rich permafrost landscapes and consists of geologically and geomorphologically diverse terraces covered with tundra vegetation and of active floodplains, featuring approximately 6 500 km of channels and over 30 000 lakes. Because of its broad landscape and habitat diversity the delta is a biodiversity hotspot with high numbers of nesting and breeding migratory birds, fish, caribou and other mammals and was designated a State Nature Reserve in 1995. Characterizing plant composition, above ground biomass and application of field spectroscopy was a major focus of a 2018 expedition to the delta. These field data collections were linked to Sentinel-2 satellite data to upscale local patterns in land cover and associated habitats to the entire delta. Here, we describe multiple field datasets collected in the Lena Delta during summer 2018 including foliage projective cover (Shevtsova et al., 2021a), above ground biomass (Shevtsova et al., 2021b), and hyperspectral field measurements (Runge et al., 2022, https://doi.pangaea.de/10.1594/PANGAEA.945982). We further describe a detailed Sentinel-2 satellite image-based classification of habitat types for the central Lena Delta (Landgraf et al., 2022), an upscaled classification for the entire Lena Delta (Lisovski et al., 2022), as well as a synthesis product for disturbance regimes (Heim and Lisovski, 2023, https://doi.org/10.5281/zenodo.7575691) in the delta that is based on the classification, the described datasets, and field expertise. We present context and detailed methods of these openly available datasets and show how they can improve our understanding of the rapidly changing Arctic tundra system. The new Lena Delta habitat distribution dataset represents a first baseline against which future observations can be compared. With the link between such detailed habitat type classifications and disturbance regimes future upscaling efforts may provide a better understanding of how Arctic lowland landscapes will respond to climate change and how this will impact land surface processes.

1 Introduction

Global warming has profound impacts on the polar regions (Serreze and Barry, 2011; Overland et al., 2019). Rapidly increasing temperatures and changing precipitation regimes result in declining sea ice, warming and thawing of permafrost, more frequent tundra fires, and changes in vegetation (e.g., Biskaborn et al., 2019; Hu et al., 2015; Mauclet et al., 2022; Box et al., 2019; Amap, 2021). The Arctic tundra biome, which is normally characterized by harsh living conditions and nutrient-deficiency, has experienced rapid phenological shifts, such as earlier green-up in spring, which is also associated with increasing shrubification rates (Mekonnen et al., 2021). Shifts in plant communities are also driven by changing nutrient availability in permafrost soils (Mekonnen et al., 2021; Mauclet et al., 2022), affecting the net primary productivity of tundra ecosystems.

Satellite-derived remote sensing can provide large-scale assessments of Arctic vegetation cover and changes therein (Bartsch et al., 2016). For example, the Circumpolar Arctic Vegetation Map (CAVM) project, from the Conservation of Arctic Flora and Fauna working group (CAFF), provided a first panarctic vegetation composition map based on Advanced Very-High Resolution Radiometer (AVHRR) false-color infrared (CIR) composites at a 1:4 million map scale (Walker, 1998; Raynolds et al., 2019). Later, higher resolution land cover maps became available across all spatial scales from national and international efforts such as the NASA Arctic-Boreal Vulnerability Experiment (ABoVE) providing open-source data collections from boreal and arctic regions (ABoVE Science Definition Team, 2014) specifically for Alaska, Canada, Northern Europe, and Western Siberia, providing a better bridge to field measurements. Such products greatly assist in monitoring and upscaling of patterns and dynamics of soil properties, land-atmosphere fluxes, ecosystem states, and changes therein (e.g., Walker, 1998; Beamish et al., 2020; Berner et al., 2020; Sweeney et al., 2022; Macander et al., 2022; Endsley et al., 2022). For selected Eastern Siberian tundra regions, land cover maps have been produced for some specific regions (e.g., Veremeeva and Gubin, 2009; Bartsch et al., 2019; Schneider et al., 2009), including the Lena Delta (Bartsch et al., 2019; Schneider et al., 2009).

Arctic river deltas represent distinct and vulnerable geomorphological and ecological regions at the marine-terrestrial boundary. River deltas have been studied intensively to better understand land cover and vegetation compositions (Jorgenson, 2000; Schneider et al., 2009; Frost et al., 2020; Bartsch et al., 2020), carbon pools and fluxes (Bartlett et al., 1992; Schneider et al., 2009; Sachs et al., 2008; Rossger et al., 2022), and land cover change caused by climate change impacts (Jorgenson, 2000; Pisaric et al., 2011; Lantz et al., 2015; Nitze and Grosse, 2016; Vulis et al., 2021; Juhls et al., 2021). With diverse habitats, Arctic river deltas are biodiversity hotspots (Gilg et al., 2000), but at the same time are prone to rapid changes (Walker, 1998; Overeem et al., 2022). Arctic deltas are affected by permafrost thaw (e.g., Pisaric et al., 2011; Nitze and Grosse, 2016; Vulis et al., 2021), sea ice loss (Overeem et al., 2022), and increased sediment transport and organic load during spring floods (Piliouras and Rowland, 2020; Juhls et al., 2021). Arctic river deltas are very dynamic systems and high-resolution habitat information from these biodiversity hotspots is needed to assess and predict changes and implications of Arctic warming.

The Lena Delta is the largest Arctic river delta representing a typical lake-rich lowland permafrost landscape (Grigoriev, 1993). Over the last decades, the central Lena Delta has been a place of intensive research. In addition to long-term permafrost monitoring projects at the Research Station Samoylov Island (Hubberten et al., 2006; Boike et al., 2019), extensive records on meteorology, soil and ecosystem characteristics (Zibulski et al., 2016; Boike et al., 2019; Boike et al., 2008), hydrology (Fedorova et al., 2015), and greenhouse gas fluxes (Rossger et al., 2022; Holl et al., 2019) are available, setting an important benchmark for further assessments of changes in an Arctic river delta. Schneider et al. (2009) developed the first land cover classification map for the entire delta at 30 m spatial resolution based on Landsat-7 satellite summer images from 2000 and 2001 to quantify delta-wide methane emissions. The increase of datasets

https://doi.org/10.5194/essd-2023-36
Preprint. Discussion started: 24 February 2023

collected within the Lena Delta enables updated classification, using higher resolution Sentinel-2 (S-2, 10 to 20 m pixel resolution) images and improved thematic detail based on extensive ground observations.

In the following study, field datasets and derived Earth Observation products based on multispectral, S-2 satellite data for the Lena Delta provide 1) an updated data-driven framework for plant communities and associated habitat classes in the Lena Delta, 2) a high-resolution habitat mapping product for the entire delta, and as an example for the application of such an habitat map 3) an upscaling of information on disturbance regimes and links to habitat types. Integrating these datasets enhances our understanding of the Lena Delta system and will build a baseline and framework for future spatio-temporal analysis of more detailed processes and changes within this highly sensitive ecosystem.

2 Study Area

The Lena Delta is located in northeastern Siberia's continuous permafrost zone between 72° and 74°N and 123° to 130°E (Figure 1). With an area of about 30 000 km^2, it is the largest delta in the Arctic and one of the largest in the world (Walker, 1998; Schneider et al., 2009). It is surrounded by the Laptev Sea to the west, north, and east, and the Chekanovsky and Kharaulakh mountain ranges border it to the south. The delta is characterized by numerous river channels and more than 1500 islands with a diverse geologic history (Grigoriev, 1993). Morphologically, the delta can be divided into three distinct geomorphological main terraces (Grigoriev, 1993; Schwamborn et al., 2002). The first main terrace, which comprises the Holocene fluvial terraces and the active floodplains, is the youngest and most active part of the delta (Schwamborn et al., 2023), and covers most of the east-northeastern areas as well as the southern and southwestern-most parts This main terrace predominantly consists of ice wedge-polygonal tundra (Nitzbon et al., 2020) as well as of barren and vegetated floodplain areas (e.g., Rossger et al., 2022). The second main terrace, located in the northwestern part, contains mostly sandy, comparably well-drained soils with low ground-ice content (Schwamborn et al., 2002; Ulrich et al., 2009). Large, mostly north-to-south oriented lakes and depressions are abundant in this area (Morgenstern et al., 2008). The third and oldest main terrace consists mainly of remnants of a Late Pleistocene accumulation plain with ice- and organic-rich sediments (so-called Yedoma deposits) and is characterized by polygonal tundra with large ice wedges, deep thermokarst lake basins, and thermo-erosional valleys (Morgenstern et al., 2011; Morgenstern et al., 2021). The third terrace is found on islands in the southern delta region (Schirrmeister et al., 2003; Schirrmeister et al., 2011). Permafrost in the area has a thickness of about 500–600 m (Romanovskii and Hubberten, 2001). The active layer depth, i.e., the seasonally thawing upper soil layer, on the first terrace is usually in the range of 30 to 50 cm and 80 to 120 cm on the floodplains (Boike et al., 2019). The larger region is characterized by an Arctic continental climate with low mean annual air temperatures of −13 °C, a mean temperature in January of −32 °C, and a

https://doi.org/10.5194/essd-2023-36
Preprint. Discussion started: 24 February 2023

mean temperature in July of 6.5 °C. The mean annual precipitation is low and amounts to about 190 mm (World Weather Information Service).

As part of past Russian-German expeditions to the Lena Delta, most research during the last two decades has been carried out on the islands of Samoylov and Kurungnakh in the central delta (Figure 1). Samoylov Island (72°22′ N, 126°29′ E) covers an area of about 5 km^2 and is representative of the first terrace together with an active floodplain (Boike et al., 2019; Boike et al., 2008). The vegetation and soil types are diverse at local scales due to high lateral variability of the polygonal microrelief consisting of drier polygon rims, and moist to wet polygonal depressions and troughs (Nitzbon et al., 2020; Kienast and Tsherkasova, 2001). In contrast, Kurungnakh Island is mainly composed of late Pleistocene Yedoma deposits that belong to the third delta terrace (Grigoriev, 1993) with elevation up to 55 m above sea level (m a.s.l.) (Morgenstern et al., 2013). Holocene cover deposits and peat-rich permafrost soils are distributed across the surface of the third Lena River terrace and especially concentrated in the deep thermokarst basins called "alases". Alases are important landscape-forming features of the ice-rich Yedoma permafrost zone, which are mainly caused by extensive melting of excess ground ice in the underlying permafrost (Van Everdingen, 1998).

3 Datasets and methods

Here, new datasets and an upscaling application are presented for the Lena Delta that are spatially and thematically connected and support vegetation, habitat, and land cover applications for this region (Figure 1).

Two datasets feature field-measured vegetation data, providing information on foliage projective cover (Dataset 1) and above ground biomass (Dataset 2) recorded in the central Lena Delta in summer 2018 across 26 selected vegetation plot sites (supplementary table S1, S2). The field plots of 30 x 30 m (900 m^2) were chosen to be representative for typical vegetation communities (vascular plants, moss and lichen cover) as largely homogenous sites representative for the surrounding area. In addition, a total of 28 in-situ, canopy-level hyperspectral field measurements were acquired in 30 x 30 m plots with homogeneous vegetation or barren to partially vegetated areas (spectral reflectance field measurements; Dataset 3). Of the 28 hyperspectral measurements, 15 were conducted at vegetation plot sites, three measurements were repeat measurements to capture vegetation senescence, and at 10 spectrometry plots we conducted hyperspectral field measurements without floristic inventories but with detailed plot documentation. Based on expert knowledge, we defined representative land cover classes and identified homogeneous regions within the central Lena Delta to train and apply a vegetation classifier using a Sentinel-2 (S2) satellite image from summer 2018 (Dataset 4). Due to the high accuracy of the central Lena Delta vegetation classification and positive evaluation by field experts, we used this vegetation classification as a training dataset for a robust classifier that was subsequently applied to a Sentinel-2 image mosaic for the entire Lena Delta for 2018 (Dataset 5).

https://doi.org/10.5194/essd-2023-36
Preprint. Discussion started: 24 February 2023

Finally, using the habitat classes, probability maps for exposed sandbars and water distribution, and information from the empirical in-situ dataset (Datasets 1 & 2), we extrapolated a classification of disturbance regimes across the delta (Dataset 6) as an application example for the habitat classes.

3.1 Foliage projective cover (Dataset 1)

A detailed description of plant composition for the 26 vegetation plots of the 2018 expedition to the Lena Delta was compiled (see supplementary table S1, S2, S3). Prior to the field work, the approximate site locations were defined for establishing representative vegetation plots based on field knowledge and Landsat and Sentinel-2 satellite imagery. The aim was to cover representative vegetation communities of the central delta. At each site location, we defined a plot centre in a 30 x 30 m square plot with a homogeneous vegetation type that was also representative of the wider land surface serving as an Elementary Sampling Unit (ESU) according to the Committee on Earth Observing Satellites Working Group on Calibration and Validation (Duncanson et al., 2021) In case of patchier vegetation, we were careful that the 30 x 30 m squares were set in a minimum of 50 x 50 m square of the same type.

First, the projective vegetation cover around the plot centre was recorded in rings of 50 cm width from the plot centre. In addition, the vegetation plot was mapped in detail from above with one Red-Green-Blue (RGB) and one Red-Green-Near Infrared (RGNIR) camera using telescope stick-based field photography. Detailed floristic composition was recorded in at least three subplots (2 x 2 m) per ground cover vegetation type inside the plot. If the ground vegetation cover was homogenous, only three subplots were established. In the case of more diverse vegetation, for example polygonal tundra with dry rims and moist to wet depressions, more subplots were established (see, Figure 2 describing the concept). We compiled the floristic composition to foliage projective cover by plant taxa on each 2 x 2 m subplot for the different canopy levels and upscaled to the 30 x 30 m plot using the field photo maps. The dataset of percentage foliage projective cover per vegetation plot is published in PANGAEA (Shevtsova et al., 2021a, https://doi.pangaea.de/10.1594/PANGAEA.935875).

3.2 Above ground plant biomass (Dataset 2)

Above-ground biomass (ABG) was sampled in the field in 25 of the 26 selected vegetation plots in 2018 (see supplementary table S1, S2, S3). Within each 2 x 2 m subplot a 0.5 x 0.5 m representative plot was selected for ABG sampling. AGB sampling for moss and lichens was conducted within 0.1 x 0.1 m subplots inside the 0.5 x 0.5 m subplots. In total, 174 fresh AGB samples were collected and weighed in the field or subsequently at the Samoylov research station. AGB samples with a weight exceeding 15 g were subsampled. The plant samples were then dried for two to four days in a warm dry place and finally oven-dried for ca. 24 hours at a temperature of 60 °C before re-weighing. All AGB assessments per plant community type were upscaled to the 30 x 30 m plot in g/m^2 using the field photo maps. The

https://doi.org/10.5194/essd-2023-36
Preprint. Discussion started: 24 February 2023

dataset of AGB per vegetation plot has been published in PANGAEA (Shevtsova et al., 2021b, https://doi.pangaea.de/10.1594/PANGAEA.935923).

3.3 Hyperspectral field measurements (Dataset 3)

Hyperspectral field measurements were conducted in the central Lena Delta in August 2018 with the aim to collect surface reflectance spectra of different homogeneous land cover units across a variety of delta land surfaces. In total, we collected 28 hyperspectral field measurements in homogeneous 30 x 30 m spectrometry plots, with 15 of them equalling the vegetation plots across Samoylov and Kurungnakh islands (see Dataset 1 & 2 *and supplementary table S4),* three as repeat measurements at the end of August to capture the change in spectral signature during senescence since the beginning of August and the remaining 10 field-spectroscopy plots focusing on non-vegetated areas such as sandy parts of the floodplain. We conducted the field-spectroscopy measurements with a Spectral Evolution SR-2500 field spectrometer with a 1.5 m Fiber Optic Cable. The instrument was calibrated to spectral radiance within a wavelength range of 350 to 2500 nm. Within the 30 x 30 m homogeneous spectrometry plots we acquired about 100 individual measurements, randomly scattered across the plot. Before and after each survey we conducted reference measurements by measuring the back reflected downwelling radiance from a Zenith Lite^{TM} Diffuse Reflectance Target of 50% reflectivity to normalize to surface reflectance percentages per wavelength. The averaged individual measurements of the reflectance of each spectrometry plot was published in the PANGAEA data repository (Runge et al., 2022, https://doi.pangaea.de/10.1594/PANGAEA.945982).

3.4 Central Lena Delta habitat classification (Dataset 4)

3.4.1 Habitat Classes

Based on the vegetation plots (Dataset 1 & 2) and from field knowledge, different habitat types characterized by distinct plant communities, moisture regimes and soil properties were defined. Non-vegetated areas (e.g., sand) and water were added as additional classes using band thresholds (Table 1). During an iterative process within the S-2 based supervised classification, additional habitat types that were not covered by the vegetation plots (Dataset 1 & 2) were added: i) polygonal tundra complex could spectrally be separated into three distinct classes related to different surface water abundance in the form of intra- and interpolygonal ponds with up to 10%, 20%, 50% surface water cover, and ii) sparsely vegetated areas as transition zones between vegetated and barren. Table 1 provides details on habitat type descriptions and established methods to distinguish habitats.

3.4.2 Satellite data processing

https://doi.org/10.5194/essd-2023-36
Preprint. Discussion started: 24 February 2023

The central Lena Delta habitat classification is based on one high quality cloudless S-2A Level 2A image from August 6 in 2018, representing the late summer. The S-2 Level-1C (top of atmosphere reflectance, TOA) image data was processed by the German Space Agency DLR (B. Pflug, oral communication, 2019) to Level-2A (bottom of atmosphere, BOA) surface reflectance using the newest version of the atmospheric correction processor Sen2Cor later released as ESA Sen2Cor in 2020. Atmospheric correction processing was performed with the default rural aerosol model. All spectral bands were resampled to the 10 m pixel resolution bands. The 60 m pixel resolution bands (B1, B9, B10) that support atmospheric correction, but are not optimal for land surface classification, were removed. We added the normalized difference vegetation index (NDVI; NIR-RED / NIR + RED) to the band collection.

3.4.3 Central delta habitat classification

The Sentinel-2 pixels from the 30 x 30 m vegetation plots, and additional polygons defined by expert knowledge, led to 8 626 training pixels for the classification. We tested several classifiers and different selected band combinations (spectral bands and NDVI). The classification was forced to express vegetation composition, biomass and moisture regimes. We omitted the water class (transparent to turbid) and the sandbank surfaces from the classification processing by masking them as inactive using a band threshold method. The water mask was based on the NIR 10 m band 8 (NIR < 0.02) and the sand mask was based on the blue 10 m band 2 (Blue > 0.07, Table 1). Best results for the habitat classification were obtained using a random forest classification with a band combination of all S-2 VIS, Red-Edge, NIR and SWIR bands, and the NDVI. The final central Lena Delta habitat classification contains 12 classes (including water and barren/sand as distinct classes, see Table 1).

The chosen classifier was able to distinguish all relevant classes (Table 1) and was even able to identify patchy habitat spots. The result of a cross-validation indicated an overall class accuracy of 96.78% (Landgraf, 2020). For the test, the training dataset, consisting of data points from the vegetation plots (Dataset 1, 2), was split in half and 4 313 pixel samples were used for a second run through the classification algorithm. The precision of each class was calculated with a confusion matrix (supplementary table S5). The published dataset of Landgraf et al. (2022, https://doi.pangaea.de/10.1594/PANGAEA.945057) provides the central Lena Delta habitat classification map and the ESUs and polygons used to train the classifier. The training dataset includes data from 23 of the 26 vegetation plots (Dataset 1, 2), as well as additional 69 ESUs defined with expert knowledge gathered during several field expeditions to the Lena Delta.

3.5 Lena Delta habitat classification (Dataset 5)

3.5.1 Lena Delta habitat classes

https://doi.org/10.5194/essd-2023-36
Preprint. Discussion started: 24 February 2023

In order to extend the habitat classification map to the entire Lena Delta, we included all the habitats covering the central delta (Dataset 4, table 1). In addition, based on expert knowledge and extensive visual satellite image investigations, we added an additional habitat type that is not present in the central Lena Delta: the second terrace in the northwest of the Lena Delta is lithologically and geomorphologically different from the other two terraces present in the central delta, and characterized by sandy substrates. In a hyperspectral CHRIS PROBA satellite-based land cover classification, Ulrich et al. (2009) described the second terrace featuring very dry elevated sandbanks, barren or poorly vegetated areas with isolated lichens, moss, herbs, dwarf shrubs or grasses (vegetation cover 0–60%, growth height: max. 20 cm, average active layer depth of 1 m on the upland plain with old, vegetation-arrested sand dunes). Based on photos taken in the field during past expeditions (see supplementary table S3) the habitat class shows well-drained areas dominated by sandy substrate and diverse, sparse vegetation cover; some areas are dominated by sedges, cotton grass and mosses with rare occurrences of lichens and dwarf shrubs, while some areas are dominated by the latter. Schneider et al. (2009) defined this class as 'dry moss-, sedge- and dwarf shrub-dominated tundra (DMSD)'. We selected 35 ESUs for this habitat class characterized by high SWIR reflectance (S-2 band 11) due to dry land surface conditions. The habitat type was named 'dwarf shrub - herb communities' and was added as an additional habitat class to the training data set.

3.5.2 Satellite data processing

The Lena Delta habitat classification was based on a Sentinel-2 mosaic (top of atmosphere (TOA) reflectance, Google Earth Engine Dataset) with images taken of the area between June 1 and September 15, 2018. The images (N = 1684) were filtered to discard images with cloud cover above 20%. A cloud mask was applied to the remaining 262 images, masking pixels where the quality band 'QA60' indicates clouds (band 10) or cirrus (band 11). All spectral bands with 20 m resolution were resampled to match the 10 m resolution bands. Next, NDVI was computed (see 3.4) for each image and one high-quality mosaic of all images based on the maximum NDVI value per pixel was produced representing a snapshot of the peak summer vegetation period. Using the median NIR band values across the 262 cloud-masked images, we classified water with a threshold of < 0.07 reflectance. The remaining non-vegetated areas defined by a threshold of NDVI < 0.4 were classified as barren/sand. The water- and sand-masked image mosaics were then used in the classification pipeline with the following bands: B2 (blue), B3 (green), B4 (red), B5 (red edge 1), B6 (red edge 2), B7 (red edge 3), B8 (NIR), B11 (SWIR 1), B12 (SWIR 2), and NDVI.

3.5.3 Lena Delta Habitat classification

Given the high accuracy and thorough validation of the central Lena Delta habitat classification (Dataset 4) we used the result to train a random forest classifier (smileRandomForest in Google Earth Engine). To this end, we selected 7500 random points within the vegetated area of the central Lena Delta (labelled according to the underlying vegetation class of Dataset 4), plus 35 ESUs selected within the 'dwarf shrub - herb communities' of the north-western Lena Delta. Visual

https://doi.org/10.5194/essd-2023-36
Preprint. Discussion started: 24 February 2023

inspection of experts found high accuracy in the spatial distribution of habitat classes across the delta. Formal validation was based on a comparison between the classification result and another random sample of 5 000 points from the training dataset (Dataset 4). In addition, and since the barren/sandy areas are highly dynamic with variable water levels mainly within (due to flooding in spring and decreasing river flow during the summer season) but also across years (discharge dynamics), we computed a sandbar probability map for the Lena Delta using cloud masked Sentinel-2 (TOA surface reflectance) images between April 1 and October 15 from 2015 to 2021 (n = 6.026 image tiles). In each image, we labelled sandy pixels by NDVI < 0.4 AND NDWI > 0.095 AND NIR < 9% reflectance. Next, for each pixel in the Lena Delta, we computed the percentage of sandy pixels across all images resulting in a sand probability map. The training dataset (random 7500 points, plus 35 points with label 'dwarf shrubs - herb communities'), the habitat classification, and the sandbar probability map was published in the PANGAEA repository (Lisovski et al., 2022, https://doi.pangaea.de/10.1594/PANGAEA.946407).

3.6 Lena Delta disturbance regimes (Dataset 6)

Mainly annual flooding, but also local rapid thaw processes on the land surface of the terraces with ice-rich permafrost, result in disturbance regimes forming distinct habitat types (Table 2). The floodplains experience seasonal flooding as a regularly occurring disturbance in spring after ice-break up (the spring flood). Very high disturbance regimes due to the most intense scour, erosion and sedimentation result in barren sandbanks or in early-stage plant communities equalling the 'sparsely vegetated' habitat class. 'moist to wet sedge communities', 'wet sedge communities', 'moist equisetum and shrubs', 'dry shrub communities', 'dry grass to wet sedge communities' forms the mid to advanced successional stages on the floodplain (high disturbance regime) with shifting habitat types according to (Stanford et al., 2005; Driscoll and Hauer, 2019).

In contrast to the floodplain, habitats on the first, second and third delta terraces are less extensively disturbed (low disturbance) allowing the development of the typical mature-state tundra plant communities: 'polygonal tundra complex', 'tussock tundra', and 'dwarsh shrub herb communities'. However, locally, high disturbance occurs by rapid thaw processes of ice-rich permafrost (first and third delta terraces) with habitats characterized by mid to advanced-stage plant succession: 'moist to wet sedge communities', 'wet sedge communities', 'dry shrub communities', and 'dry grass to wet sedge' communities. Very high disturbance due to intense rapid thaw processes occurs at eroding cliffs and lake margins, in steep valleys and actively developing gullies resulting in barren surfaces with rims of sparsely vegetated transition zones. Given the link between plant communities and flooding as well as rapid thaw processes, we characterised the disturbance regimes for each habitat class (Table 2) and provide an upscaling product in the form of a disturbance map for the entire Lena Delta (Heim and Lisovski, 2023, https://doi.org/10.5281/zenodo.7575691).

https://doi.org/10.5194/essd-2023-36
Preprint. Discussion started: 24 February 2023

4 Results and Discussion

We deliver a detailed description and associated data products of the most prominent habitat classes in the largest Arctic river delta, the Lena Delta. Combining ecological field data of plant composition, hyperspectral field measurements from the same sites, regional expert knowledge collected over decades, as well as S-2 satellite data, allowed us to develop a high-resolution habitat map for the entire delta. The compiled datasets and analyses provide the necessary baseline for future investigations of the biochemical processes, ecological dynamics, and responses to global warming within the Arctic tundra system of the delta.

4.1 Habitat classes

Based on the floristic composition and biomass of the vegetation plots (Dataset 1, 2), the spectral properties from hyperspectral field measurements (Dataset 3) and S-2 satellite data, as well as expert knowledge, we defined 11 distinct habitat classes linked to different vegetation composition for the Lena Delta (Figure 3). The selected S-2 spectral bands and the derived NDVI values allow a separation of the habitat classes into two distinct groups (hierarchical level 1, Figure 3a). Three habitat classes (‘wet sedge communities’, ‘moist Equisetum and shrub communities’, ‘dry grass to wet sedge communities’) formed in areas of high disturbance by rapid thaw processes and regular flooding represent a distinct cluster with highest vegetation vitality (high NDVI), and separated from the more stable and mature tundra communities (‘polygonal tundra complex’, ‘dry (tussock) tundra’, and ‘dry dwarf-shrub and herb communities’), and the other successional plant communities *(‘*moist to wet sedge complex’, ‘dry low shrub communities’ and ‘sparsely vegetated’) all characterised by a lower NDVI range. The ‘dry dwarf-shrub and herb communities’ form a separate cluster with the least overlap with other habitat types within the two-dimensional non-metric multidimensional scaling (NMDS) space (hierarchical level 2, Figure 3a; Figure 3c) due to very low vegetation vitality and surface moisture (lowest NDVI, high red and SWIR reflectance). There are two remaining habitat classes on the 3rd and 4th hierarchical level, which are successional plant communities, the ‘moist to wet sedge complex*’* and ‘dry low shrub communities’. The separation on the 3rd and 4th hierarchical level is mainly driven by higher NDVI of these successional plant community classes in comparison with the mature state tundra plant communities with lower NDVI (Figure 3a/b). The ‘dry grass to wet sedge communities’ and the ‘sparsely vegetated area’ habitat type (not covered by vegetation plots but added during the classification process), show the largest overlap with the other habitat types due to a high variability in vegetation cover, biomass and moisture. In general, the ordination method (Figure 3b) shows that distinct plant communities and the associated habitat classes are mostly separated by a biomass gradient for which the NDVI is a good approximator. A further separation linked to potential spectral proxies for biomass exists with the far red-edge and NIR bands (B6,7,8) but is less distinct than the NDVI axis. Together with the SWIR (B11,12) the red (B4) and near red-edge (B5) bands,

https://doi.org/10.5194/essd-2023-36
Preprint. Discussion started: 24 February 2023

and less strongly the blue and green bands (B2,3), the results indicate a habitat class separation based on moisture, biomass and vegetation colour characteristics.

The vegetation plot selection was made in relation to the most typical habitats (e.g., Mueller-Bombois and Ellenberg, 1974). For 15 of the 26 vegetation plots, we collected and provide hyperspectral surface reflectance data (Runge et al., 2021). These measurements cover a variety of landscape units including Yedoma uplands, floodplains (vegetated and non-vegetated), drained thermokarst lake basins (old and recently drained), and areas covered by low shrub layers. Comparing the hyperspectral surface reflectance with multispectral S-2 data, we found commonalities in the discrimination of habitat classes along moisture gradients. Unfortunately, the hyperspectral field measurements do not cover the biomass gradient. Plot measurements with the field spectrometer are conducted with the hand-held instrument held at shoulder height, hence it was not possible to acquire field spectroscopy measurements in disturbed patches with tall shrubs or very sloped terrain. This highlights the difficulty in deriving high spectral resolution surface reflectance measurements representative of fine scale differences between Arctic tundra habitat classes if the plot conditions become too challenging to measure.

In general, mature-state tundra plant communities have relatively similar spectral properties due to low vascular plant cover (e.g., Beamish et al., 2017). In addition, the tundra vegetation communities contain a wide range of accessory pigment composition (carotenoids and anthocyanins) that result in a very similar spectral response (Beamish et al., 2018). Only the highly disturbed communities such as wetlands or areas with tall shrubs are more spectrally distinct due to a high NIR reflectance plateau (Buchhorn et al., 2013). Since the hyperspectral field measurements provide a higher spatial resolution and thus also a measure of variability within areas of the same general habitat type, we consider the measurements valuable for applications that aim at analysing ecological and biochemical processes within distinct habitats in more detail.

4.2 Habitat class mapping

The identified habitat classes (Table 1) in the central Lena Delta were mapped with S-2 satellite data and a random forest classifier, achieving an overall class accuracy of 96.78% (Dataset 4). Additionally, the classification contains a water and a sand class, which were derived separately based on band masking thresholds. The central Lena Delta classification depicts both the different vegetation types, such as 'wet sedge', 'dry tundra' and 'dry shrub communities', but also the varying moisture regimes and surface water contributions, for example for the 'polygonal tundra complex' in the central delta.

Polygonal tundra is characterized by high spatial heterogeneity; at the meter-scale plant composition and diversity is defined by the polygonal microrelief and water level (Whitaker and Woodwell, 1968; Forman and Godron, 1981; Zibulski et al., 2016; Nitzbon et al., 2020). Therefore, within a single S-2 pixel, dry polygonal rims, moist slopes, wet patches and surface water can all be present. The spatial resolution of S-2 cannot capture the meter-scale, but captures the heterogeneity between the different surface water contributions of the 'polygonal tundra complex' on the first and third terrace. Field expertise and expert knowledge were key to accomplish the classification and verify its high accuracy.

The central Lena Delta classification was the basis for a delta-wide classification (Figure 5a, Dataset 5). We defined ESUs for the missing habitat class on the second terrace, produced an optimized standardized input dataset (S-2, Jun-Sept 2018), and applied the best performing classification algorithm (random forest classifier), to obtain a similarly high classification accuracy (98.6 % within the central Lena Delta), covering all three geomorphological terraces.

The habitat map shows the ice-rich first and third terraces mainly covered by i) the 'polygonal tundra complex' due to impeded drainage on the terrace plateaus and by ii) drier tundra communities on well drained areas due to older degraded permafrost forms (detailed description in Morgenstern et al., 2008, 2011). On the second terrace, the classified 'dry dwarf shrub and herb communities' occur well separated from the moist habitat classes covering the floor of the alases. On the floodplains, the rich mosaic outlines a wide spectrum of very diverse classes, the dry versus moist and wet substrate habitats, in the active delta area.

In the Lena Delta, the 'polygonal tundra complex with up to 50% surface water' represents the dominant habitat class with 25% of the delta area (about 7 434 km^2). All other habitat classes represent 1-6% of the delta area with 'dwarf shrub-herb communities' and 'moist to wet sedge complex' reaching 5.4% and 5.9%, respectively (Figure 5). Based on the summer S-2 mosaic, the classes 'Water' and 'Sand' cover more than 40% of the delta. However, those two classes are extremely variable within and across years, depending on the river water level during image acquisition time. To provide information on this variability, we calculated how often each pixel in the delta (cloud free S-2 pixels from 2015 to 2022) was classified as sand (threshold approach). This led to an additional sand probability layer with values between 0-100%.

Despite extensive research within the area, only a few classification products are available for the Lena Delta. The new Lena Delta classification is a high-resolution (Sentinel-2, 10 m) map that focuses on the delta-specific habitat classes and emphasizes the high level of heterogeneity across the delta. We compared the Lena Delta habitat classification to existing classifications: the first published Lena Delta-wide land cover classification targeted towards tundra environments and the upscaling of methane emissions with 30 m resolution (Schneider et al., 2009), the global ESA Climate Change Initiative land cover classification with 300 m resolution (Defourny, 2019), and a circum-arctic standardized ESA GlobPermafrost land cover map of the Lena Delta with 20 m resolution (Bartsch et al., 2019). We sampled the classification results with a regular point grid of more than 3 million points which have an equal distance of 100 m to one another to compare the classification results. Figures and tables with more information on class comparisons can be found in the supplements (Table XX, Figure S3, S4m, S5). Overall, the classifications of the Lena Delta overlap well for 'water' (water bodies (Defourny, 2019), shallow water (Schneider et al., 2009), water (different depths and

https://doi.org/10.5194/essd-2023-36
Preprint. Discussion started: 24 February 2023

sediment yields, Bartsch et al. 2019)) and 'sand' (bare areas (Defourny, 2019), mainly non-vegetated areas (Schneider et al., 2009), sand, seasonally inundated and disturbed (Bartsch et al. 2019)) areas. Besides this, the mapped classes differ greatly from one another. For example, the dominant classes in the coarse ESA CCI land cover 2018 product (300 m) for the Lena Delta are 'shrub or herbaceous cover', 'flooded', 'fresh / saline / brackish water', 'sparse vegetation (tree, shrub, herbaceous cover) (<15%)', and 'mosaic tree and shrub (>50%)', 'herbaceous cover (>50%)'.

These broad classes describe the major land cover in the Arctic delta but fail to depict the heterogeneity of habitats and plant communities not only because of its coarse spatial resolution but also because of the broad class descriptions. Furthermore, smaller areas are classified as 'tree cover', 'needleleaved', 'evergreen / deciduous', 'closed to open (>15%)' and 'mosaic tree and shrub (>50%) / herbaceous cover (<50%)' which is an inaccurate depiction of the delta.

This habitat map and the land cover classification from Schneider et al. (2009) resemble each other more closely, however, this habitat map shows more differentiation in the classes and spatial resolution, 10 m to 30 m, respectively. The only class description that is identical in both classifications, besides water and sand / mainly non-vegetated areas, is 'dry tussock tundra'. However, there is only a small match between these classes in the point comparison (Fig. Sx) and most 'dry tussock tundra' areas from the Schneider et al. (2009) classification fall into the PC_50%:, PC_20%, 'moist wet sedge complex' and 'dwarsh shrub-herb communities'. The habitat map shows the mosaic of habitats on the floodplain with 'moist equisetum and shrubs on floodplain', 'dry low shrub community', 'moist to wet sedge' and 'wet sedge complex' which match with 'moist to dry dwarf shrub-dominated tundra' in the land cover classification of Schneider et al. (2009). Also, for the polygonal tundra complex, our habitat map shows more differentiation with three classes of up to 50% 20% 10% surface water contribution versus two classes in Schneider et al. (2009) 'wet sedge and moss dominated tundra' and 'moist grass and moss dominated tundra' The areas covered by 'PC_50%' and 'PC_20%' match with 'wet sedge- and moss-dominated tundra', and 'PC_20%' and 'PC_10%' match with 'moist grass and moss-dominated tundra'. The overall aim of both maps is to differentiate between dry to wet land cover types/habitats as these describe the heterogeneity in the delta well and determine factors related to methane emissions (see Schneider et al. 2009) and the different habitat classes.

The land cover classification from ESA GlobPermafrost differentiates between 21 classes which are associated to eight broader groups, such as sparse vegetation, shrub tundra, forest, grassland, floodplain, disturbed, barren and water (Bartsch et al., 2019). With a spatial resolution of 20 m, the latter product is the closest to this habitat map. The major class 'wet ecotopes' of ESA GlobPermafrost match with our 'PC_50%:' on the first terrace and the 'moist to wet sedge complex' on the floodplains. On the floodplain however, other classes show less agreement. The ESA GlobPermafrost one class 'floodplain mostly fluvial' does not differentiate the floodplain classes further, in contrast to our habitat map differentiating beweeen 'moist to wet sedge complex', 'wet sedge complex', 'moist equisetum and shrubs' and 'dry low shrub community' on floodplain. Whereas the ESA GlobPermafrost class 'disturbed' (defined as forest fire scars,

https://doi.org/10.5194/essd-2023-36
Preprint. Discussion started: 24 February 2023

seasonally inundation and landslide scars can be found in 'PC_50%' predominantly, in 'sand', 'PC_20%' and 'sparsely vegetated areas' in our habitat map, This underlines the complex structure of match and mismatch between classifications.

The habitat map gives a highly accurate and detailed description of the Arctic Lena Delta that incorporates extensive field data and expert knowledge. The habitat map is superior to the ESA CCI land cover map (2018) in both spatial resolution and class description as it depicts the heterogeneous habitat distribution. The 20m ESA GlobPermafrost classification matches the resolution of the habitat map closely but due to its wider geographical application with circum-Arctic standardized classes it does not optimally represent Lena Delta-specific habitats, such as the widely distributed polygonal tundra complex. Furthermore, the habitat map is an update to Schneider et al. (2009), which was based on three Landsat images from 2000 and 2001 and shows further differentiation of habitats, specifically representing the floodplain mosaics of this Arctic delta.

4.2 Habitat linked disturbance regimes

Parts of the Lena Delta are characterised by disturbances due to annual floodings or rapid permafrost thaw processes leading to specific habitat classes. We provide an upscaling product of habitat linked disturbance regimes (describing the type and intensity of disturbances) across the delta. Our product (Dataset 6, Figure 5a) shows that the largest part of the vegetated delta (excluding 12 439 km^2 of 'sand' and 'water' classes) is impacted by low disturbance, resulting in mature-state plant communities on the terrace plateaus (Figure 5b, 72%, 12 806 km^2). Specifically, the second terrace in the northwest of the delta, with low ice content, is least impacted by rapid thaw processes and not part of the active delta. In contrast, the habitats in the active delta are all linked to high disturbance (27%, 4 875 km^2). The 'moist to wet sedge complex*'* (10% of the vegetated Lena Delta) is the largest class considered to be formed by high disturbance. This class is found in larger patch sizes on the riverine floodplains, smaller patches on the floor of thermo-erosional valleys. Overall, 27.5% of the vegetated area of the Lena Delta experiences some level of high disturbance from either regular spring floods or from rapid thaw processes.

Species richness, relative abundance and biomass characteristics are important habitat features that are influenced by landscape characteristics such as topography, water fluxes, soil types and disturbance regimes (Forman and Godron, 1981; Naiman et al., 1986; Pickett et al., 1989; Montgomery, 1999). Greig-Smith (1964), Woodwell and Whittaker (1968), and Forman and Godron (1981) described fragmentation of land surfaces due to disturbance (defined by type and intensities) and topography. In the Lena Delta, the terrace-related topography and active floodplain areas are major determinants of plant communities and habitat classes and are thus well reflected in the Lena Delta habitat map.

The high disturbance regime on floodplains results in 'shifting habitats' (Stanford et al., 2005; Driscoll and Hauer, 2019). The annual spring floods and rapid thaw processes result in areas of high disturbances, habitats of mid to advanced plant successional stages showing high vascular plant above ground biomass (Figure 5c) due to the higher nutrient availability, a deeper active layer and more moisture (e.g., Myers-Smith et al., 2020). Within the low disturbance habitat classes, a thick moss layer as well as a low vascular plant coverage characterise the tundra community assemblages representing mature state plant communities. Because high disturbance patches are characterized by high vascular biomass, they can be well classified specifically in the NDVI, but also NIR and red edge bands of optical medium resolution sensors such as S2. Within the vegetation plots (Dataset 1), we did not find clear differences in species richness and in the Shannon diversity index between the disturbed and the undisturbed classes (Figure 5d). Since most disturbed habitat classes such as the 'moist to wet sedge', the 'wet sedge' as well as homogeneous patches of high shrubs (as part of the habitat class 'dry grass to wet sedge complex'), were not sampled in the field due to too challenging conditions, however they are clearly representing habitats with low species richness. In the extreme case disturbance can lead to barren and sparsely vegetated surfaces.

5 Conclusions

The described datasets provide coherent and complementary information of the major habitat classes in the Lena Delta in Arctic Siberia, the largest delta in the Arctic. Based on extensive knowledge collected during fieldwork that included habitat-related measurements of plant composition, biomass, and hyperspectral field measurements we provide a validated and high-resolution habitat classification map of the delta. In addition, we linked ecologically important characteristics of disturbances in the delta to habitat classes, providing a baseline for future studies of Arctic change as well as a foundation for potential upscaling of related processes such as biodiversity, ecosystem functions, and biochemical dynamics such as greenhouse gas emissions. With this update of previous land cover and habitat-related mapping products of the Lena Delta we strive to facilitate and promote future investigations leading to a better understanding of this highly sensitive arctic delta system.

Acknowledgements

Field work in the Lena River Delta was conducted in the frame of the Russian-German LENA Expeditions based at Research Station Samoylov Island. We thank all colleagues and station staff involved in the organization and logistics for their great support.

Code/Data availability

Dataset 1: (Shevtsova et al., 2021a, https://doi.pangaea.de/10.1594/PANGAEA.935875)

https://doi.org/10.5194/essd-2023-36
Preprint. Discussion started: 24 February 2023

Dataset 2: (Shevtsova et al., 2021b, https://doi.pangaea.de/10.1594/PANGAEA.935923)

Dataset 3: (Runge et al., 2022, https://doi.pangaea.de/10.1594/PANGAEA.945982)

Dataset 4: (Landgraf et al., 2022, https://doi.pangaea.de/10.1594/PANGAEA.945057)

Dataset 5: (Lisovski et al., 2022, https://doi.pangaea.de/10.1594/PANGAEA.946407)

Dataset 6: (Heim and Lisovski, 2023, https://doi.org/10.5281/zenodo.7575691)

Competing interests

Birgit Heim is a member of the editorial board of ESSD. Otherwise, we declare no competing interests.

Funding

SL acknowledges funding from the Geo.X Network for Geosciences in Berlin and Brandenburg. This study was supported by BMBF KoPf (Grant Number 03F0764B), KoPf Synthesis (Grant Number 03F0834B), and AWI base funds. AR was partially funded by ESA GlobPermafrost and an ESA CCI postdoctoral fellowship. BH acknowledges HGF REKLIM

Authors contribution

SL: Conceptual framework, habitat classification, data analysis, writing

AR: Conceptual framework, field work, spectral field data collection, habitat classification, spectral data processing, data analysis, writing

IS: Field work, data collection, concept of biomass sampling, habitat classification

RRO: Habitat classification

NL: Habitat classification, spectral data processing

MF: Field work, spectral field data collection

NL: habitat definition

AM: Project management, writing

AB: Protocol and code for field spectrometry processing

CS: Field spectrometry processing

GG: Project management, habitat classification, writing

UH: Project management, concept of vegetation & biomass sampling, co-supervision of field data analyses

BH: Conceptual framework, habitat classification, project management, field work, data collection, writing

References

AMAP: AMAP Arctic Climate Change Update 2021: Key Trends and Impacts. Arctic Monitoring and Assessment Programme (AMAP), Tromsø, Norway, viii+148pp, 2021.

Bartlett, K. B., Crill, P. M., Sass, R. L., Harriss, R. C., and Dise, N. B.: Methane Emissions from Tundra Environments in the Yukon-Kuskokwim Delta, Alaska, Journal of Geophysical Research-Atmospheres, 97, 16645-16660, Doi 10.1029/91jd00610, 1992.

Bartsch, A., Hofler, A., Kroisleitner, C., and Trofaier, A. M.: Land Cover Mapping in Northern High Latitude Permafrost Regions with Satellite Data: Achievements and Remaining Challenges, Remote Sensing, 8, ARTN 979
10.3390/rs8120979, 2016.

Bartsch, A., Widhalm, B., Pointner, G., Ermokhina, K., Leibman, M., and Heim, B.: Landcover derived from Sentinel-1 and Sentinel-2 satellite data (2015-2018) for subarctic and arctic environments [dataset], https://doi.org/10.1594/PANGAEA.897916, 2019.

Bartsch, A., Widhalm, B., Leibman, M., Ermokhina, K., Kumpula, T., Skarin, A., Wilcox, E. J., Jones, B. M., Frost, G. V., Hofler, A., and Pointner, G.: Feasibility of tundra vegetation height retrieval from Sentinel-1 and Sentinel-2 data, Remote Sensing of Environment, 237, ARTN 111515
10.1016/j.rse.2019.111515, 2020.

Beamish, A., Raynolds, M. K., Epstein, H., Frost, G. V., Macander, M. J., Bergstedt, H., Bartsch, A., Kruse, S., Miles, V., Tanis, C. M., Heim, B., Fuchs, M., Chabrillat, S., Shevtsova, I., Verdonen, M., and Wagner, J.: Recent trends and remaining challenges for optical remote sensing of Arctic tundra vegetation: A review and outlook, Remote Sensing of Environment, 246, ARTN 111872
10.1016/j.rse.2020.111872, 2020.

Beamish, A. L., Coops, N., Chabrillat, S., and Heim, B.: A Phenological Approach to Spectral Differentiation of Low-Arctic Tundra Vegetation Communities, North Slope, Alaska, Remote Sensing, 9, ARTN 1200
10.3390/rs9111200, 2017.

Beamish, A. L., Coops, N. C., Hermosilla, T., Chabrillat, S., and Heim, B.: Monitoring pigment-driven vegetation changes in a low-Arctic tundra ecosystem using digital cameras, Ecosphere, 9, ARTN e02123
10.1002/ecs2.2123, 2018.

Berner, L. T., Massey, R., Jantz, P., Forbes, B. C., Macias-Fauria, M., Myers-Smith, I., Kumpula, T., Gauthier, G., Andreu-Hayles, L., Gaglioti, B. V., Burns, P., Zetterberg, P., D'Arrigo, R., and Goetz, S. J.: Summer warming explains widespread but not uniform greening in the Arctic tundra biome, Nature Communications, 11, ARTN 4621
10.1038/s41467-020-18479-5, 2020.

Biskaborn, B. K., Smith, S. L., Noetzli, J., Matthes, H., Vieira, G., Streletskiy, D. A., Schoeneich, P., Romanovsky, V. E., Lewkowicz, A. G., Abramov, A., Allard, M., Boike, J., Cable, W. L., Christiansen, H. H., Delaloye, R., Diekmann, B., Drozdov, D., Etzelmuller, B., Grosse, G., Guglielmin, M., Ingeman-Nielsen, T., Isaksen, K., Ishikawa, M., Johansson, M., Johannsson, H., Joo, A., Kaverin, D., Kholodov, A., Konstantinov, P., Kroger, T., Lambiel, C., Lanckman, J. P., Luo, D. L., Malkova, G., Meiklejohn, I., Moskalenko, N., Oliva, M., Phillips, M., Ramos, M., Sannel, A. B. K., Sergeev, D., Seybold, C., Skryabin, P., Vasiliev, A., Wu, Q. B., Yoshikawa, K., Zheleznyak, M., and Lantuit, H.: Permafrost is warming at a global scale, Nature Communications, 10, ARTN 264
10.1038/s41467-018-08240-4, 2019.

Boike, J., Wille, C., and Abnizova, A.: Climatology and summer energy and water balance of polygonal tundra in the Lena River Delta, Siberia, Journal of Geophysical Research-Biogeosciences, 113, Artn G03025
10.1029/2007jg000540, 2008.

Boike, J., Nitzbon, J., Anders, K., Grigoriev, M., Bolshiyanov, D., Langer, M., Lange, S., Bornemann, N., Morgenstern, A., Schreiber, P., Wille, C., Chadburn, S., Gouttevin, I., Burke, E., and Kutzbach, L.: A 16-year record (2002-2017) of permafrost, active-layer, and meteorological conditions at the Samoylov Island Arctic permafrost research site, Lena River delta, northern Siberia: an opportunity to validate remote-sensing data and land surface, snow, and permafrost models, Earth System Science Data, 11, 261-299, 10.5194/essd-11-261-2019, 2019.

Box, J. E., Colgan, W. T., Christensen, T. R., Schmidt, N. M., Lund, M., Parmentier, F. J. W., Brown, R., Bhatt, U. S., Euskirchen, E. S., Romanovsky, V. E., Walsh, J. E., Overland, J. E., Wang, M. Y., Corell, R. W., Meier, W. N., Wouters, B., Mernild, S., Mard, J., Pawlak, J., and Olsen, M. S.: Key indicators of Arctic climate change: 1971-2017, Environmental Research Letters, 14, ARTN 045010
10.1088/1748-9326/aafc1b, 2019.

Buchhorn, M., Walker, D. A., Heim, B., Raynolds, M. K., Epstein, H. E., and Schwieder, M.: Ground-Based Hyperspectral Characterization of Alaska Tundra Vegetation along Environmental Gradients, Remote Sensing, 5, 3971-4005, 2013.

Defourny, P.: ESA Land Cover Climate Change Initiative (Land_Cover_cci): Global Land Cover Maps, Version 2.0.7 [dataset], 2019.

Driscoll, K. P. and Hauer, F. R.: Seasonal flooding affects habitat and landscape dynamics of a gravel-bed river floodplain, Freshwater Science, 38, 510-526, 10.1086/704826, 2019.

Duncanson, L., Armston, J., Disney, M., Avitabile, V., Barbier, N., Calders, K., Carter, S., Chave, J., Herold, M., MacBean, N., McRoberts, R., Minor, D., Paul, K., Réjou-Méchain, M., Roxburgh, S., Williams, M., Albinet, C., Baker, T., Bartholomeus, H., Bastin, J. F., Coomes, D., Crowther, T., Davies, S., de Bruin, S., De Kauwe, M., Domke, G., Dubayah, R., Falkowski, M., Fatoyinbo, L., Goetz, S., Jantz, P.,

https://doi.org/10.5194/essd-2023-36
Preprint. Discussion started: 24 February 2023

Jonckheere, I., Jucker, T., Kay, H., Kellner, J., Labriere, N., Lucas, R., Mitchard, E., Morsdorf, F., Næsset, E., Park, T., Phillips, O. L., Ploton, P., Puliti, S., Quegan, S., Saatchi, S., Schaaf, C., Schepaschenko, D., Scipal, K., Stovall, A., Thiel, C., Wulder, M. A., Camacho, F., Nickeson, J., Román, M., and Margolis, H.: Aboveground Woody Biomass Product Validation Good Practices Protocol. Version 1.0, Land Product Validation Subgroup (WGCV/CEOS), doi:10.5067/doc/ceoswgcv/lpv/agb.001, 2021.

Endsley, K. A., Kimball, J. S., and Reichle, R. H.: Soil Respiration Phenology Improves Modeled Phase of Terrestrial net Ecosystem Exchange in Northern Hemisphere, Journal of Advances in Modeling Earth Systems, 14, ARTN e2021MS002804 10.1029/2021MS002804, 2022.

Fedorova, I., Chetverova, A., Bolshiyanov, D., Makarov, A., Boike, J., Heim, B., Morgenstern, A., Overduin, P. P., Wegner, C., Kashina, V., Eulenburg, A., Dobrotina, E., and Sidorina, I.: Lena Delta hydrology and geochemistry: long-term hydrological data and recent field observations, Biogeosciences, 12, 345-363, 10.5194/bg-12-345-2015, 2015.

Forman, R. T. T. and Godron, M.: Patches and Structural Components for a Landscape Ecology, Bioscience, 31, 733-740, Doi 10.2307/1308780, 1981.

Frost, G. V., Loehman, R. A., Saperstein, L. B., Macander, M. J., Nelson, P. R., Paradis, D. P., and Natali, S. M.: Multi-decadal patterns of vegetation succession after tundra fire on the Yukon-Kuskokwim Delta, Alaska, Environmental Research Letters, 15, ARTN 025003 10.1088/1748-9326/ab5f49, 2020.

Gilg, O., Sané, R., Solovieva, D. V., Pozdnyakov, V. I., Sabard, B., Tsanos, D., Zöckler, C., Lappo, E. G., Syroechkovski, J. E. E., and Eichhorn, G.: Birds and Mammals of the Lena Delta Nature Reserve, Siberia, ARCTIC, 53, 118-133, 10.14430/arctic842, 2000.

Greig-Smith, P.: Quantitative plant ecology, Butterworths1964.

Grigoriev, M. N.: Crio Morphogenesis in the Lena Delta, Permafrost Institute Press, Yakutsk1993.

Heim, B. and Lisovski, S.: Lena Delta habitat disturbance regimes (0.0) [dataset], https://doi.org/10.5281/zenodo.7575691, 2023.

Holl, D., Wille, C., Sachs, T., Schreiber, P., Runkle, B. R. K., Beckebanze, L., Langer, M., Boike, J., Pfeiffer, E. M., Fedorova, I., Bolshianov, D. Y., Grigoriev, M. N., and Kutzbach, L.: A long-term (2002 to 2017) record of closed-path and open-path eddy covariance CO2 net ecosystem exchange fluxes from the Siberian Arctic, Earth System Science Data, 11, 221-240, 10.5194/essd-11-221-2019, 2019.

Hu, F. S., Higuera, P. E., Duffy, P., Chipman, M. L., Rocha, A. V., Young, A. M., Kelly, R., and Dietze, M. C.: Arctic tundra fires: natural variability and responses to climate change, Frontiers in Ecology and the Environment, 13, 369-377, 10.1890/150063, 2015.

Hubberten, H.-W., Wagner, D., Pfeiffer, E.-M., Boike, J., and Gukov, A. Y.: The Russian-German research station samoylov, Lena delta - A key site for polar research in the Siberian arctic, Polarforschung, 2006.

Jorgenson, M. T.: Hierarchial organisation of ecosystems at multiple spatial scales on the Yukon-Kuskokwim Delta, Alaska, USA, Arctic Antarctic and Alpine Research, 32, 221-239, Doi 10.2307/1552521, 2000.

Juhls, B., Antonova, S., Angelopoulos, M., Bobrov, N., Grigoriev, M., Langer, M., Maksimov, G., Miesner, F., and Overduin, P. P.: Serpentine (Floating) Ice Channels and their Interaction with Riverbed Permafrost in the Lena River Delta, Russia, Frontiers in Earth Science, 9, ARTN 689941 10.3389/feart.2021.689941, 2021.

Kienast, F. and Tsherkasova, J.: Comparative botanical recent-studies in the Lena River Delta [Field Report], Alfred Wegener Institute, Germany, 2001.

Landgraf, N., Shevtsova, I., Pflug, B., and Heim, B.: Sentinel-2 derived central Lena Delta land cover classification [dataset], https://doi.pangaea.de/10.1594/PANGAEA.945057, 2022.

Lantz, T. C., Kokelj, S. V., and Fraser, R. H.: Ecological recovery in an Arctic delta following widespread saline incursion, Ecological Applications, 25, 172-185, 10.1890/14-0239.1, 2015.

Lisovski, S., Runge, A., Okoth, R. R., Shevtsova, I., and Heim, B.: Lena Delta Land Cover Classification (2018, Sentinel-2), PANGAEA [dataset], https://doi.pangaea.de/10.1594/PANGAEA.946407, 2022.

Lorang, M. S. and Hauer, F. R.: Fluvial geomorphic processes, in: Methods in stream ecology, edited by: Hauer, F. R., and Lamberti, G. A., Academic Press/Elsevier, San Diego, 145–168, 2006.

Macander, M. J., Nelson, P. R., Nawrocki, T. W., Frost, G. V., Orndahl, K. M., Palm, E. C., Wells, A. F., and Goetz, S. J.: Time-series maps reveal widespread change in plant functional type cover across Arctic and boreal Alaska and Yukon, Environmental Research Letters, 17, ARTN 054042 10.1088/1748-9326/ac6965, 2022.

Mauclet, E., Agnan, Y., Hirst, C., Monhonval, A., Pereira, B., Vandeuren, A., Villani, M., Ledman, J., Taylor, M., Jasinski, B. L., Schuur, E. A. G., and Opfergelt, S.: Changing sub-Arctic tundra vegetation upon permafrost degradation: impact on foliar mineral element cycling, Biogeosciences, 19, 2333-2351, 10.5194/bg-19-2333-2022, 2022.

Mekonnen, Z. A., Riley, W. J., Berner, L. T., Bouskill, N. J., Torn, M. S., Iwahana, G., Breen, A. L., Myers-Smith, I. H., Criado, M. G., Liu, Y. L., Euskirchen, E. S., Goetz, S. J., Mack, M. C., and Grant, R. F.: Arctic tundra shrubification: a review of mechanisms and impacts on ecosystem carbon balance, Environmental Research Letters, 16, ARTN 053001 10.1088/1748-9326/abf28b, 2021.

Montgomery, D. R.: Process domains and the river continuum, Journal of the American Water Resources Association, 35, 397-410, DOI 10.1111/j.1752-1688.1999.tb03598.x, 1999.

Morgenstern, A., Grosse, G., and Schirrmeister, L.: Genetic, morphological, and statistical characterization of lakes in the permafrost-dominated Lena Delta, Ninth International Conference on Permafrost2008.

Morgenstern, A., Grosse, G., Gunther, F., Fedorova, I., and Schirrmeister, L.: Spatial analyses of thermokarst lakes and basins in Yedoma landscapes of the Lena Delta, Cryosphere, 5, 849-867, 10.5194/tc-5-849-2011, 2011.

Morgenstern, A., Overduin, P. P., Gunther, F., Stettner, S., Ramage, J., Schirrmeister, L., Grigoriev, M. N., and Grosse, G.: Thermo-erosional valleys in Siberian ice-rich permafrost, Permafrost and Periglacial Processes, 32, 59-75, 10.1002/ppp.2087, 2021.

Morgenstern, A., Ulrich, M., Gunther, F., Roessler, S., Fedorova, I. V., Rudaya, N. A., Wetterich, S., Boike, J., and Schirrmeister, L.: Evolution of thermokarst in East Siberian ice-rich permafrost: A case study, Geomorphology, 201, 363-379, 10.1016/j.geomorph.2013.07.011, 2013.

Mueller-Bombois, D. and Ellenberg, H.: Aims and methods of vegetation ecology, Wohn Wiley & Sons, New York, USA1974.

Myers-Smith, I. H., Kerby, J. T., Phoenix, G. K., Bjerke, J. W., Epstein, H. E., Assmann, J. J., John, C., Andreu-Hayles, L., Angers-Blondin, S., Beck, P. S. A., Berner, L. T., Bhatt, U. S., Bjorkman, A. D., Blok, D., Bryn, A., Christiansen, C. T., Cornelissen, J. H. C., Cunliffe, A. M., Elmendorf, S. C., Forbes, B. C., Goetz, S. J., Hollister, R. D., de Jong, R., Loranty, M. M., Macias-Fauria, M., Maseyk, K., Normand, S., Olofsson, J., Parker, T. C., Parmentier, F. J. W., Post, E., Schaepman-Strub, G., Stordal, F., Sullivan, P. F., Thomas, H. J. D., Tommervik, H., Treharne, R., Tweedie, C. E., Walker, D. A., Wilmking, M., and Wipf, S.: Complexity revealed in the greening of the Arctic, Nature Climate Change, 10, 106-117, 10.1038/s41558-019-0688-1, 2020.

Naiman, R. J., Melillo, J. M., and Hobbie, J. E.: Ecosystem Alteration of Boreal Forest Streams by Beaver (Castor-Canadensis), Ecology, 67, 1254-1269, Doi 10.2307/1938681, 1986.

Nitzbon, J., Westermann, S., Langer, M., Martin, L. C. P., Strauss, J., Laboor, S., and BOike, J.: Fast response of cold ice-rich permafrost in northeast Siberia to a warming climate, Nature Communications, 11, ARTN 2201 10.1038/s41467-020-15725-8, 2020.

Nitze, I. and Grosse, G.: Detection of landscape dynamics in the Arctic Lena Delta with temporally dense Landsat time-series stacks, Remote Sensing of Environment, 181, 27-41, 10.1016/j.rse.2016.03.038, 2016.

Obu, J., Westermann, S., Barboux, C., Bartsch, A., Delaloye, R., Grosse, G., Heim, B., Hugelius, G., Irrgang, A., Kääb, A. M., Kroisleitner, C., Matthes, H., Nitze, I., Pellet, C., Seifert, F. M., Strozzi, T., Wegmüller, U., Wieczorek, M., and Wiesmann, A.: ESA permafrost Climate Change Initiative (permafrost_cci): Permafrost extent for the Northern Hemisphere, v2.0 [dataset], https://doi.org/10.5285/28E889210F884B469D7168FDE4B4E54F, 2020.

Overeem, I., Nienhuis, J. H., and Piliouras, A.: Ice-dominated Arctic deltas, Nature Reviews Earth & Environment, 3, 225-240, 10.1038/s43017-022-00268-x, 2022.

Overland, J., Dunlea, E., Box, J. E., Corell, R., Forsius, M., Kattsov, V., Olseng, M. S., Pawlak, J., Reiersen, L. O., and Wang, M. Y.: The urgency of Arctic change, Polar Science, 21, 6-13, 10.1016/j.polar.2018.11.008, 2019.

Pickett, S. T. A., Kolasa, J., Armesto, J. J., and Collins, S. L.: The Ecological Concept of Disturbance and Its Expression at Various Hierarchical Levels, Oikos, 54, 129-136, Doi 10.2307/3565258, 1989.

Piliouras, A. and Rowland, J. C.: Arctic River Delta Morphologic Variability and Implications for Riverine Fluxes to the Coast, Journal of Geophysical Research-Earth Surface, 125, ARTN e2019JF005250 10.1029/2019JF005250, 2020.

Pisaric, M. F. J., Thienpont, J. R., Kokelj, S. V., Nesbitt, H., Lantz, T. C., Solomon, S., and Smol, J. P.: Impacts of a recent storm surge on an Arctic delta ecosystem examined in the context of the last millennium, Proceedings of the National Academy of Sciences of the United States of America, 108, 8960-8965, 10.1073/pnas.1018527108, 2011.

Raynolds, M. K., Walker, D. A., Balser, A., Bay, C., Campbell, M., Cherosov, M. M., Daniels, F. J. A., Eidesen, P. B., Emiokhina, K. A., Frost, G. V., Jedrzejek, B., Jorgenson, M. T., Kennedy, B. E., Kholod, S. S., Lavrinenko, I. A., Lavrinenko, O. V., Magnusson, B., Matveyeva, N. V., Metusalemsson, S., Nilsen, L., Olthof, I., Pospelov, I. N., Pospelova, E. B., Pouliot, D., Razzhivin, V., Schaepman-Strub, G., Sibik, J., Telyatnikov, M. Y., and Troeva, E.: A raster version of the Circumpolar Arctic Vegetation Map (CAVM), Remote Sensing of Environment, 232, ARTN 111297 10.1016/j.rse.2019.111297, 2019.

Romanovskii, N. N. and Hubberten, H. W.: Results of permafrost modelling of the lowlands and shelf of the Laptev Sea region, Russia, Permafrost and Periglacial Processes, 12, 191-202, 10.1002/ppp.387, 2001.

Rossger, N., Sachs, T., Wille, C., Boike, J., and Kutzbach, L.: Seasonal increase of methane emissions linked to warming in Siberian tundra, Nature Climate Change, 12, 1031-+, 10.1038/s41558-022-01512-4, 2022.

Runge, A., Fuchs, M., Shevtsova, I., Landgraf, N., Heim, B., Herzschuh, U., and Grosse, G.: Hyperspectral field spectrometry of Arctic vegetation units in the central Lena Delta [dataset], https://doi.org/10.1594/PANGAEA.945982, 2022.

Sachs, T., Wille, C., Boike, J., and Kutzbach, L.: Environmental controls on ecosystem-scale CH4 emission from polygonal tundra in the Lena River Delta, Siberia, Journal of Geophysical Research-Biogeosciences, 113, Artn G00a03 10.1029/2007jg000505, 2008.

https://doi.org/10.5194/essd-2023-36
Preprint. Discussion started: 24 February 2023

Open Access Earth System Science Data Discussions

Schirrmeister, L., Grosse, G., Schwamborn, G., Andreev, A. A., Meyer, H., Kunitsky, V. V., Kuznetsova, T. V., Dorozhkina, M. V., Pavlova, E. Y., Bobrov, A. A., and Oezen, D.: Late Quaternary History of the Accumulation Plain North of the Chekanovsky Ridge (Lena Delta, Russia): A Multidisciplinary Approach, Polar Geography, 27, 277-319, 10.1080/789610225, 2003.

Schirrmeister, L., Grosse, G., Schnelle, M., Fuchs, M., Krbetschek, M., Ulrich, M., Kunitsky, V., Grigoriev, M., Andreev, A., Kienast, F., Meyer, H., Babiy, O., Klimova, I., Bobrov, A., Wetterich, S., and Schwamborn, G.: Late Quaternary paleoenvironmental records from the western Lena Delta, Arctic Siberia, Palaeogeography Palaeoclimatology Palaeoecology, 299, 175-196, 10.1016/j.palaeo.2010.10.045, 2011.

Schneider, J., Grosse, G., and Wagner, D.: Land cover classification of tundra environments in the Arctic Lena Delta based on Landsat 7 ETM+ data and its application for upscaling of methane emissions, Remote Sensing of Environment, 113, 380-391, 10.1016/j.rse.2008.10.013, 2009.

Schwamborn, G., Rachold, V., and Grigoriev, M. N.: Late Quaternary sedimentation history of the Lena Delta, Quaternary International, 89, 119-134, Pii S1040-6182(01)00084-2
Doi 10.1016/S1040-6182(01)00084-2, 2002.

Schwamborn, G., Schirrmeister, L., Mohammadi, A., Meyer, H., Kartoziia, A., Maggioni, F., and Strauss, J.: Fluvial and permafrost history of the lower Lena River, north-eastern Siberia, over late Quaternary time, Sedimentology, 70, 235-258, 10.1111/sed.13037, 2023.

Serreze, M. C. and Barry, R. G.: Processes and impacts of Arctic amplification: A research synthesis, Global and Planetary Change, 77, 85-96, 10.1016/j.gloplacha.2011.03.004, 2011.

, last

Shevtsova, I., Laschinskiy, N., Heim, B., and Herzschuh, U.: Foliage projective cover of 26 vegetation sites of central Lena Delta from 2018 [dataset], https://doi.pangaea.de/10.1594/PANGAEA.935875, 2021a.

Shevtsova, I., Heim, B., Runge, A., Fuchs, M., Melchert, J., and Herzschuh, U.: Total above-ground biomass of 25 vegetation sites of central Lena Delta from 2018 [dataset], https://doi.pangaea.de/10.1594/PANGAEA.935923, 2021b.

Stanford, J. A., Lorang, M. S., and Hauer, F. R.: The shifting habitat mosaic of river ecosystems, SIL Proceedings, 1922-2010, 29, 123-136, 10.1080/03680770.2005.11901979, 2005.

Sweeney, C., Chatterjee, A., Wolter, S., McKain, K., Bogue, R., Conley, S., Newberger, T., Hu, L., Ott, L., Poulter, B., Schiferl, L., Weir, B., Zhang, Z., and Miller, C. E.: Using atmospheric trace gas vertical profiles to evaluate model fluxes: a case study of Arctic-CAP observations and GEOS simulations for the ABoVE domain, Atmospheric Chemistry and Physics, 22, 6347-6364, 10.5194/acp-22-6347-2022, 2022.

Ulrich, M., Grosse, G., Chabrillat, S., and Schirrmeister, L.: Spectral characterization of periglacial surfaces and geomorphological units in the Arctic Lena Delta using field spectrometry and remote sensing, Remote Sensing of Environment, 113, 1220-1235, 10.1016/j.rse.2009.02.009, 2009.

van Everdingen, R. O.: Multi-language glossary of permafrost and related ground-ice terms, Arctic Institute of North America University of Calgary, Calgary, Canada1998.

Veremeeva, A. and Gubin, S.: Modern Tundra Landscapes of the Kolyma Lowland and their Evolution in the Holocene, Permafrost and Periglacial Processes, 20, 399-406, 10.1002/ppp.674, 2009.

Vulis, L., Tejedor, A., Zaliapin, I., Rowland, J. C., and Foufoula-Georgiou, E.: Climate Signatures on Lake And Wetland Size Distributions in Arctic Deltas, Geophysical Research Letters, 48, ARTN e2021GL094437
10.1029/2021GL094437, 2021.

Walker, H. J.: Arctic deltas, Journal of Coastal Research, 14, 718–738, 1998.

Whitaker, R. H. and Woodwell, G. M.: Dimension, and Production Relations of Trees and Shrubs in the Brookhaven Forest, New York., Journal of Ecology, 56, 1-25, https://doi.org/10.1038/2325, 1968.

Zibulski, R., Herzschuh, U., and Pestryakova, L. A.: Vegetation patterns along micro-relief and vegetation type transects in polygonal landscapes of the Siberian Arctic, Journal of Vegetation Science, 27, 377-386, 10.1111/jvs.12356, 2016.

https://doi.org/10.5194/essd-2023-36
Preprint. Discussion started: 24 February 2023

Figures

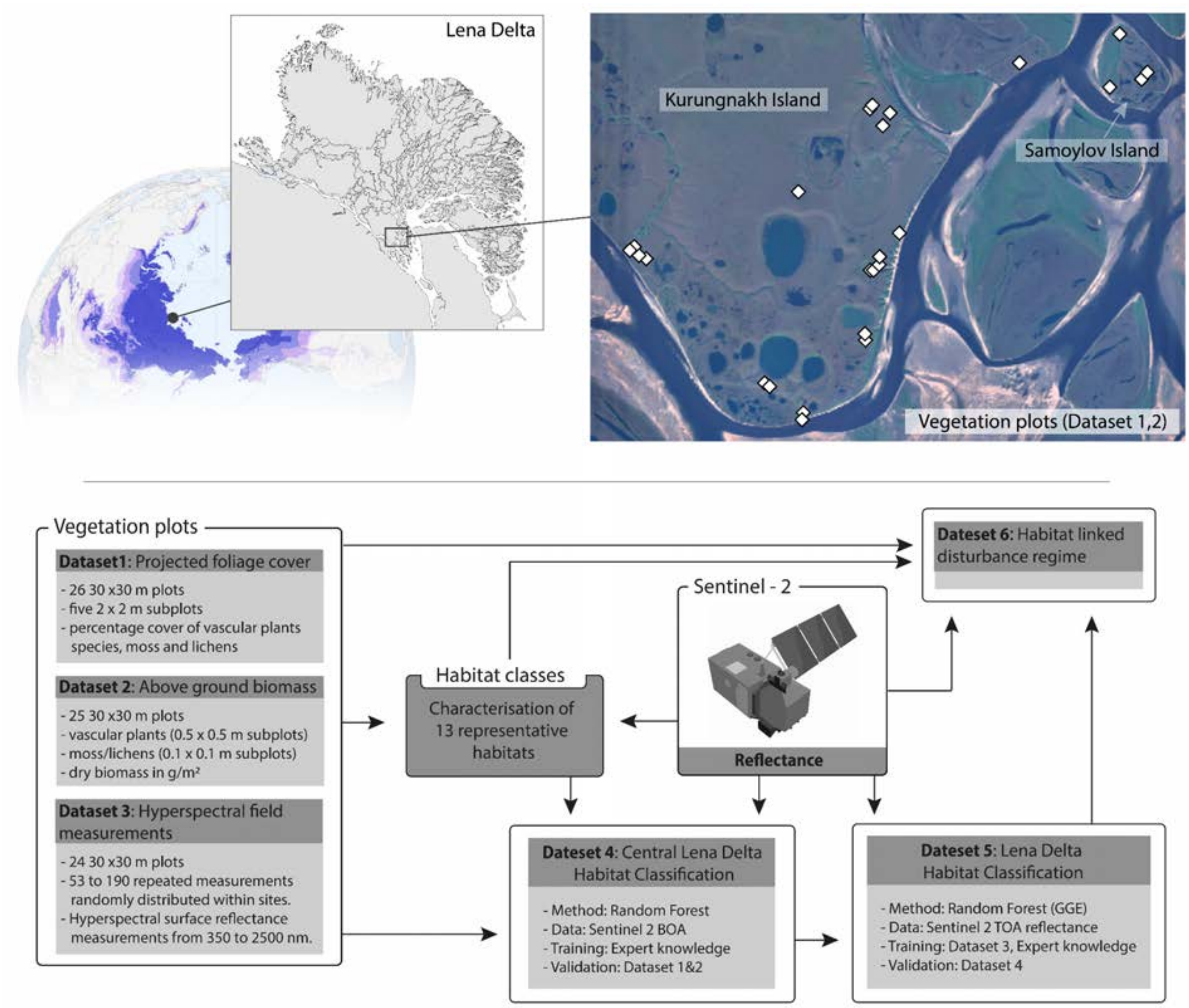

Figure 1: Geographic location of the Lena Delta in the Russian High Arctic (72.91ºN, 126.90ºE) and a Sentinel-2 RGB image (August 2018, bands 4-3-2) of the central Lena Delta showing the areas of the 26 vegetation plots where foliage projective cover and above ground biomass was determined. Panarctic overview map shows permafrost extent (colour scale indicates permafrost extent from continuous (dark purple) to isolated (light purple) (Obu et al., 2020). The grey-coloured Lena Delta land map created with Sentinel-1 water mask from Juhls et al. (2021). Bottom: Dataset characteristics and methodological links between the different datasets.

https://doi.org/10.5194/essd-2023-36
Preprint. Discussion started: 24 February 2023

Open Access Earth System Science Data Discussions

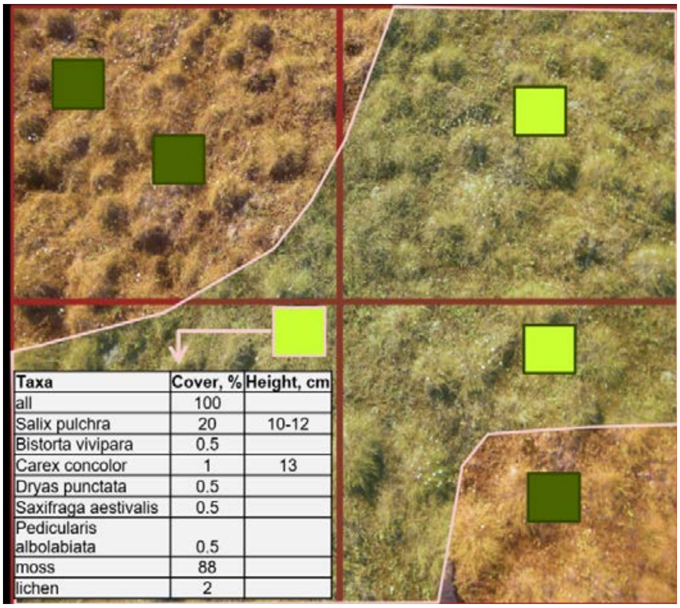

Figure 2: Schematic 30 x 30 m vegetation plot set up with 2 x 2 m subplots for vegetation cover estimation for different canopy layers and above ground biomass sampling on 0.5 x 0.5m inside the 2 x 2 m subplots. The background photo shows a vegetation plot within the tussock tundra, a relatively homogenous vegetation class that would account for one class only. Schematically we here added green and red polygons that would define sub-vegetation classes, e.g., with different moisture regimes).

https://doi.org/10.5194/essd-2023-36
Preprint. Discussion started: 24 February 2023

Open Access Earth System Science Data Discussions

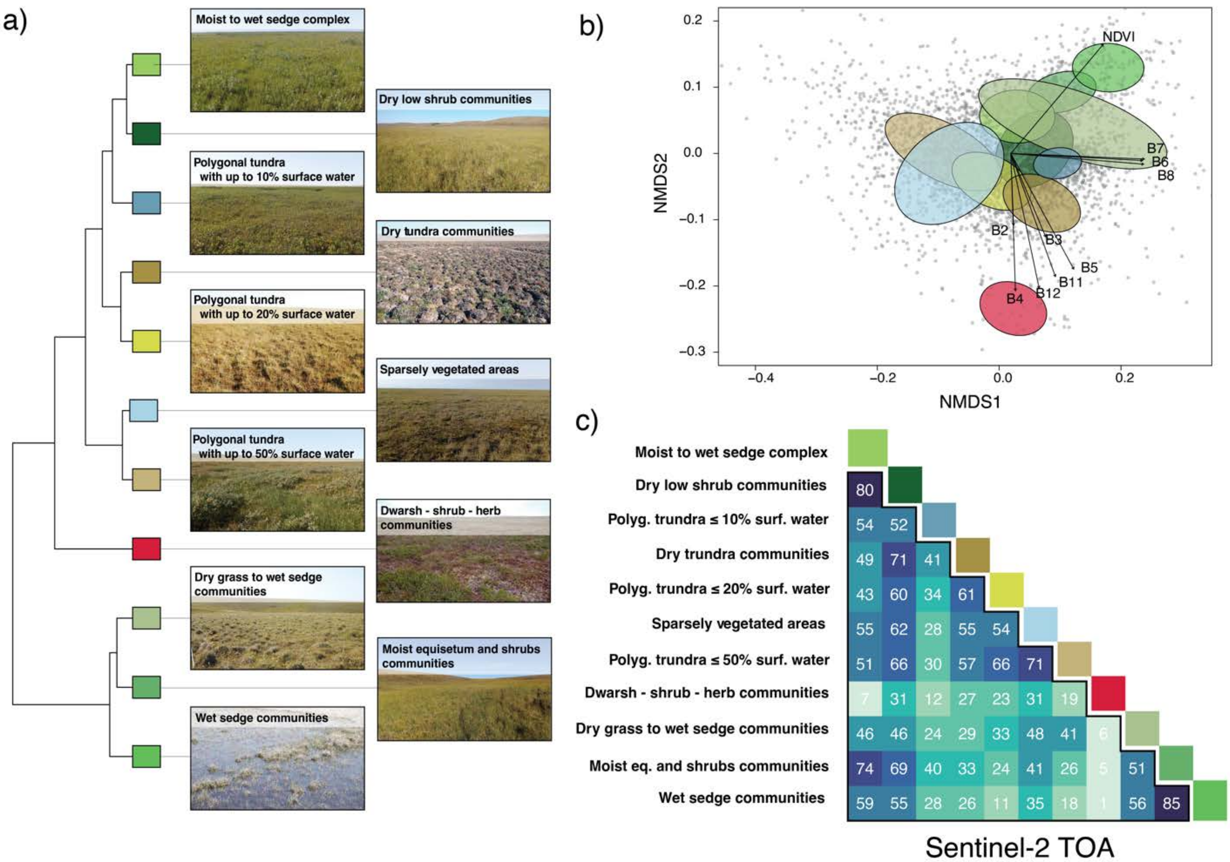

Figure 3: Similarity of habitat classes based on Sentinel-2 spectral reflectance and NDVI values. The dendrogram in panel a) indicates the multidimensional hierarchical similarity of the classes based on Sentinel-2 top of atmosphere reflectance (bands 2-8, 10-12, and NDVI). Panel b) shows the location of the habitat classes within a two-dimensional NMDS space. The arrows with the Sentinel-2 bands and NDVI indicate the correlation of these variables across the two axes. The lower matrix of panel c) depicts the calculated percentage overlap of 3,500 pixels (grey dots in panel b) across the two NMDS axes of panel b).

https://doi.org/10.5194/essd-2023-36
Preprint. Discussion started: 24 February 2023

Open Access Earth System Science Data Discussions

735

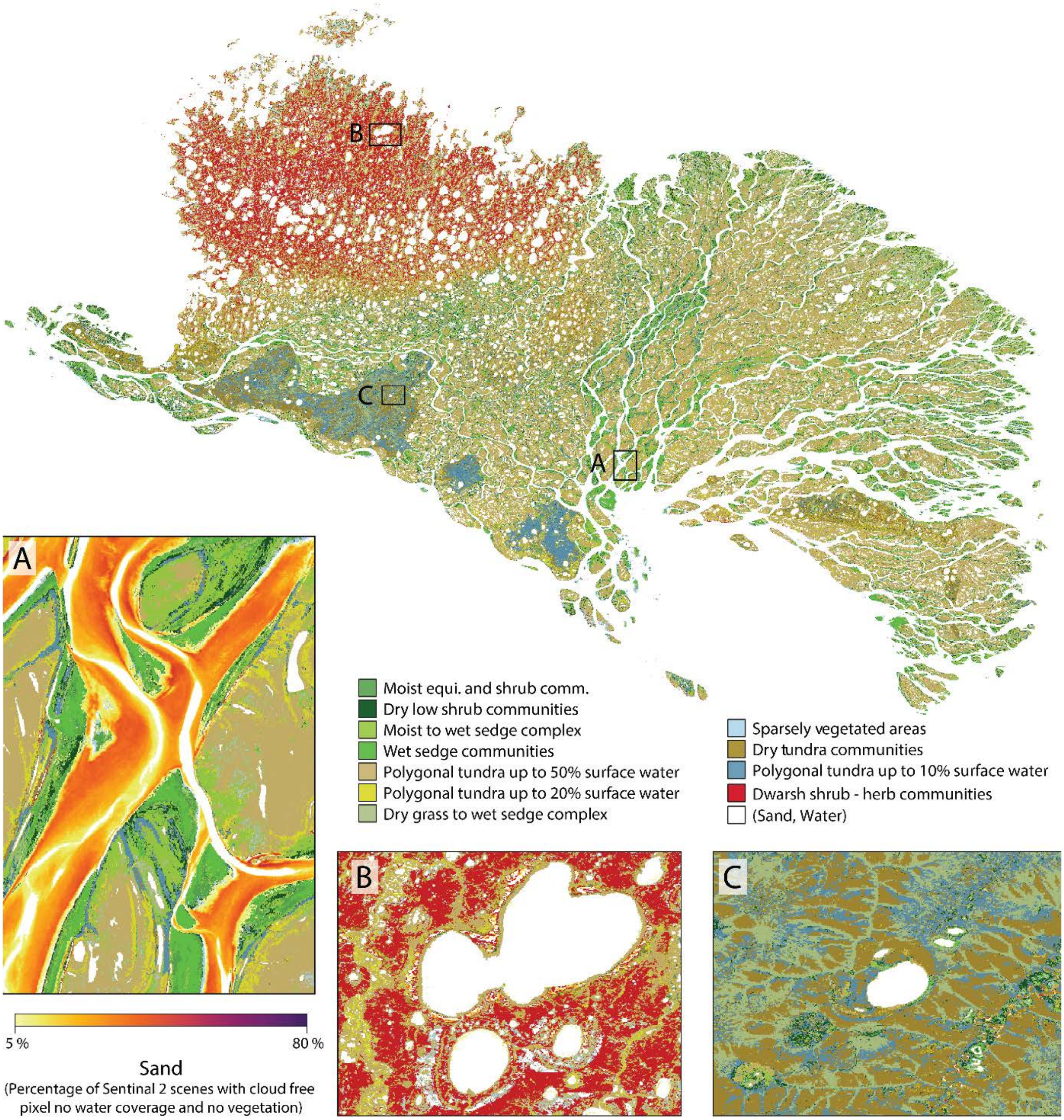

Figure 4: Lena Delta habitat classes (Dataset 5). The entire Lena Delta on the left with three regional examples (A,B,C) includes the seasonal sand probability map.

https://doi.org/10.5194/essd-2023-36
Preprint. Discussion started: 24 February 2023

Open Access Earth System Science Data Discussions

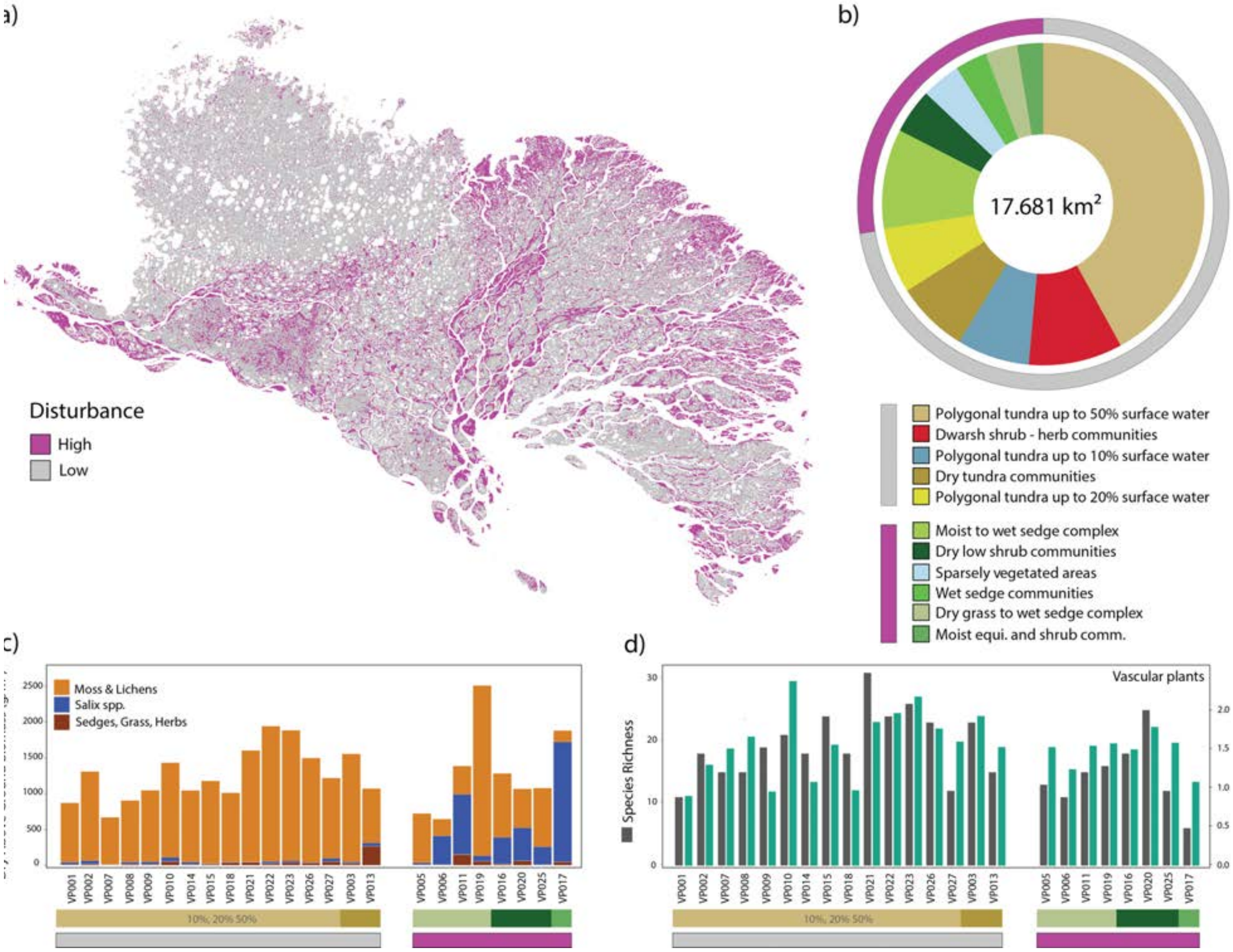

Figure 5: Habitat linked disturbance regimes across the Lena Delta. The map (a) includes all vegetated areas (excluding water and sand). The pie chart (b) shows the contribution of vegetated classes across the Lena Delta grouped by high and low disturbance regimes. The bottom panels show c) the measured dry above ground biomass (Dataset 2) and d) the species richness and Shannon index (from Dataset 1) of the vegetation plots for different habitat classes and disturbance regimes.

https://doi.org/10.5194/essd-2023-36
Preprint. Discussion started: 24 February 2023

Tables

Table 1: Habitat types, descriptions as well as methods used to characterize the distinct habitats. In-situ vegetation plot numbers correspond to the vegetation plots of Dataset 1 and 2 (see also Table S1, S2, S3).

Habitat types	Description	Method
Moist *Equisetum* and shrubs	*Equisetum* and shrub communities form a early-to-middle successional stage growing on the active floodplain. Low moss contribution	In-situ vegetation plot (VP17); extended to representative larger polygon shape files using field knowledge.
Dry shrub communities	Patch forming shrub communities dominated by dwarf willow (*Salix*) thickets, frequently occurring on dry elevated areas on floodplains and stream floodplains and in topographically sheltered areas below basin and valley rims. Low moss contribution	In-situ vegetation plots (VP04, VP16); extended to representative larger polygon shape files using field knowledge.
Polygonal tundra complex up to - 10% - 20% - 50% surface water (3 distinct classes)	Mature-state plant communities dominated by sedge, moss and herb species. Sparse vascular plant coverage (dwarf willows, dwarf birches) on thick continuous moss cover. Occurring on the plateaus of the ice-rich holocene and pleistocene terraces, and at the bottom of alases. Intersected by intra- and interpolygonal ponds resulting in up to 10%, 20%, 50% surface water contribution.	In-situ vegetation plots (VP01, VP02, VP07, VP08, VP14, VP15, VP18, VP21, VP22, VP23, VP26, VP27); extended to representative larger polygon shape files using field knowledge. The different surface water contributions were defined based on the result from unsupervised classification.
Dry grass to wet sedge communities	These early-to-middle successional plant communities cover unstable valley slopes and a yound drined lake basin, they are mostly composed of sedges and grasses, but also willows (*Salix)* are part of this habitat.	In-situ vegetation plots (VP05, VP06, VP11, VP19, VP20); extended to representative larger polygon shape files using field knowledge.
Dry tundra communities	The mature-state dry tundra communities represent the zonal tundra type, one subclass is dominated by tussock forming *Eriophorum* and the other by less tussock forming dry-herb	In-situ vegetation plots (VP03, VP13) extended to representative, larger polygon shape files using field knowledge (including 'dry

https://doi.org/10.5194/essd-2023-36
Preprint. Discussion started: 24 February 2023

Earth System Science Data Discussions
Open Access

	communities, dominated by *Dryas*. Occurring on well-drained slopes of valleys and alases, and other well-drained areas on the terraces. High moss contribution	tundra communities type tussock' and 'dry tundra communities').
Moist to wet sedge communities	These mid to advanced successional plant communities occur on moist to water-logged soils characteristically mostly in topographic depressions on the floodplains, in valleys and alases. They constitute the rims of the wetland areas on the floodplains in more dynamic parts the moss ground cover is missing.	Polygon shape files derived from high resolution satellite image and ESRI GE with regional expert knowledge. No vegetation plots (too wet).
Wet sedge communities	These mid to advanced successional plant communities occur at permanently wet sites with stagnant water in the topographic depressions and are typical for wetland areas on the floodplains. In more dynamic parts the moss ground cover is missing.	Polygon shape files derived from high resolution satellite image and ESRI GE with regional expert knowledge. No vegetation plots (too wet).
Sparsely vegetated areas	These early successional plant communities are characterized by low vegetation establishment and coverage. No to low moss contribution	Defined based on the result from unsupervised classification, polygon shape files. No vegetation plots.
Barren/Sand	Representing the wide-open sand flats of the floodplain and barren ground on valley slopes or along cliffs. In a few cases, this class represents vegetation-free bedrock outcrops.	Threshold using high reflectance in S2-band 2 blue.
Water	Represents all surface water bodies in the delta: the Lena River with river branches, streams, lakes and large ponds.	Threshold using low reflectance in S2-band 8 NIR.

Table 2: Habitat class and description of disturbance regimes and the component stand structure in form of contributions of vascular plants, and moss to total biomass. * (Driscoll and Hauer, 2019; Stanford et al., 2005), ** (Lorang and Hauer, 2006).

Habitat class	Disturbance regime	Stand structure

https://doi.org/10.5194/essd-2023-36
Preprint. Discussion started: 24 February 2023

Moist *Equisetum* and shrubs	**High; regular (annually), predicted** - spring floodings, - shifting habitat * - advanced-stage regeneration **	high vascular plant growth, low abundance of moss & lichens.
Dry shrub communities	**High; mixed disturbance types**: -regular spring floodings -rapid thaw processes (permafrost degradation) - shifting habitat - advanced-stage regeneration	high vascular plant growth, low abundance of moss.
Polygonal tundra complex	**Low; mixed disturbance types** - low for most of the habitat, except for actively eroding shores of ponds and channels - mature-state plant community	low vascular plant growth, high abundance of moss.
Dry grass to wet sedge communities	**High; mixed disturbance types**: - regular spring floodings - rapid thaw processes (permafrost degradation) - shifting habitat - advanced-stage regeneration	high vascular plant biomass, low abundance of moss.
Dry tundra communities	**Low; mixed disturbance types** - low for most of the habitat - mature-state plant community	low vascular plant biomass high abundance of moss.
Moist to wet sedge communities	**High; mixed disturbance types**: - regular spring floodings - rapid thaw processes (permafrost degradation) - shifting habitat - mid to advanced-stage regeneration	high vascular plant biomass Almost impossible to measure in-situ biomass (wet conditions and difficult access).
Wet sedge communities	**High; mixed disturbance types**: - regular spring floodings - rapid thaw processes (permafrost degradation) - shifting habitat - mid to advanced-stage regeneration	high vascular plant biomass. Almost impossible to measure in-situ biomass (wet conditions and difficult access).
Dwarf shrub herb communities	**Low; mixed disturbance types** - low for most of the habitat - mature-state plant community	low vascular plant biomass, high abundance of moss.
Sparsely vegetated areas	**Very high; mixed disturbance types** - regular spring floodings - rapid thaw processes (permafrost degradation) - shifting habitat - early-stage regeneration	lowest vascular plant biomass, no moss.

Sand banks/barren	**Very high: mixed disturbance types** - regular spring floodings - rapid thaw processes (permafrost degradation) - shifting habitat - no regeneration	Barren, constant shifting of sediments and movement of soils.